Evolution Letters, 2026, **00**(0), qrag039
https://doi.org/10.1093/evlett/qrag039
Letter

OXFORD

Invasion of new adaptive zones retains telltale signs of directional selection at macroevolutionary scales in mammals

Fabio A. Machado [1], Anna Penna [2], Diogo Melo [3], Barbara A. Costa [4], Thiago M. G. Zahn [5], Ana C. Pavan [6], Arthur Porto [7], Harley Sebastião[3], Daniela M. Rossoni [4], Gabriel Marroig [3], Alex Hubbe [8]

[1]Department of Biology, Oklahoma State University, Stillwater, OK, United States
[2]Natural History Museum at the University of Oslo, Blindern, Norway
[3]Departamento de Genética e Biologia Evolutiva, Instituto de Biociências, Universidade de São Paulo, São Paulo SP, Brazil
[4]Department of Biology, Lund University, Lund, Sweden
[5]Departamento de Linguística, Faculdade de Filosofia, Letras e Ciências Humanas, Universidade de São Paulo, São Paulo SP, Brazil
[6]Programa de Pós-Graduação em Ecologia e Evolução, Universidade Federal de São Paulo, Diadema - SP, CEP, Brazil
[7]Florida Museum of Natural History, Gainesville, FL, United States
[8]Departamento de Oceanografia, Instituto de Geociências, Universidade Federal da Bahia, Salvador, BA, Brazil
Corresponding author: Department of Biology, Oklahoma State University, Stillwater, OK 74078, United States. Email: fabio.machado@okstate.edu

Abstract

Directional selection is often viewed as a transient force in macroevolution, with its signal eroded over time by stabilizing and fluctuating selection. Yet, transitions into new adaptive zones are predicted to impose strong and sustained selective pressures that may leave a detectable signature even across deep timescales. We test this prediction by comparing the rates of multivariate skull morphological evolution required to traverse the boundaries between adaptive zones against genetic drift expectations. Our dataset includes 11,793 specimens spanning 231 species from 12 mammalian clades, each containing unique ecological transitions into new adaptive zones. Using a quantitative genetics framework, we estimated the phenotypic distances between ancestral and derived adaptive zones and contrasted them with null expectations under genetic drift. While a few adaptive zone invasions (e.g., marsupials and rodents) are consistent with drift, most exhibit substantially elevated rates of evolution. These results suggest that directional selection has recurrently shaped mammalian cranial evolution during major ecological shifts. We propose that adaptive zone transitions represent evolutionary contexts in which adaptation leaves a persistent macroevolutionary signal, challenging the prevailing view that long-term patterns are dominated by static forces.

Keywords morphological evolution, mammals, morphometrics, adaptive radiation

Introduction

A central challenge in macroevolution is determining when large-scale phenotypic divergence preserves a signal of directional selection. Although directional selection is widely invoked to explain adaptive phenotypic change, its signature is expected to become increasingly difficult to detect over long timescales. This difficulty partly arises from (1) limitations of the tools used to identify directional selection and (2) the dynamics inherent to macroevolutionary data. Quantitative genetics methods typically infer evolutionary processes by contrasting empirical rates of phenotypic divergence with null expectations under genetic drift (Houle et al., 2017; Lande, 1985; Lynch, 1990; Turelli et al., 1988). However, macroevolutionary studies have shown a negative correlation between rates of evolution and the time period in which they are calculated, meaning that the longer the time span, the lower the rate of evolution is expected to be (Gingerich, 1987, 1983, 2001; Holstad et al., 2024). As a consequence, the signal of directional selection is expected to become increasingly obscured over time, making it difficult to distinguish it from changes generated by drift or stabilizing selection.

This pattern is consistent with the view that macroevolution is governed by adaptive landscape dynamics. Under this view, species remain strongly attracted to species-specific adaptive peaks until significant environmental shifts force changes in the distribution of peaks themselves (Hansen, 1997, 2024; Simpson, 1944; Uyeda et al., 2011). Because episodes of directional change are generally brief relative to the time spent evolving around adaptive optima (Eldredge & Gould, 1972; Simpson, 1944), rates of phenotypic evolution calculated over longer time intervals tend to

Received: 24 December 2025. **Revised:** 18 July 2026. **Accepted:** 14 August 2026
© The Author(s) 2026. Published by Oxford University Press on behalf of The Society for the Study of Evolution (SSE) and European Society for Evolutionary Biology (ESEB).
This is an Open Access article distributed under the terms of the Creative Commons Attribution-NonCommercial License (https://creativecommons.org/licenses/by-nc/4.0/), which permits non-commercial re-use, distribution, and reproduction in any medium, provided the original work is properly cited. For commercial re-use, please contact reprints@oup.com for reprints and translation rights for reprints. All other permissions can be obtained through our RightsLink service via the Permissions link on the article page on our site-for further information please contact journals.permissions@oup.com

Downloaded from academic.oup.com/evlett/advance-article/doi/10.1093/evlett/qrag039/8863744 by Maria Mestriner user on 30 October 2026

decrease as they become dominated by periods of relative stasis, effectively erasing the signal of directional selection (Dzeverin, 2008; Lemos et al., 2001; Lynch, 1990; Machado et al., 2022; Porto et al., 2015; Uyeda et al., 2011). This effectively limits the usefulness of standard quantitative genetics approaches in macroevolutionary studies, especially for studying the signal of directional selection, leading to an emphasis on more phenomenological models of evolution that are less explicitly grounded in microevolutionary theory (Hansen, 1997).

While this emphasis on peak dynamics as the prevailing force has dominated the phylogenetic comparative methods literature (Hansen, 1997; Lynch, 1990; Uyeda et al., 2011), some studies did apply quantitative genetic methods to investigate macroevolutionary change directly. Most of these studies come from the biological anthropology/paleontology and primatology literature, in which rates of morphological evolution are compared with expectations derived from microevolutionary models. Studies of the divergence among human populations (Lynch, 1990; Roseman & Weaver, 2007; Roseman, 2004; Smith, 2011), between humans and Neanderthals (Weaver et al., 2007, 2008; Weaver & Stringer, 2015), during the evolution of the *Australopithecus-Homo* lineage (Schroeder et al., 2014), among higher apes [Hominidae; (Schroeder & von Cramon-Taubadel, 2017)], and across the primate order (Latrille et al., 2024; Machado et al., 2023) have reported rates of phenotypic divergence often consistent with drift and, in some cases, indicative of directional selection

Investigations of this kind outside of primates have been limited and produced mixed results. Evaluations of morphological evolution in bats (Dzeverin, 2008) and marsupials (Lemos et al., 2001; Porto et al., 2015) found rates of evolution lower than the expectation under genetic drift. A study on the evolution of Cingulata also found that rates were mostly slower than expected under drift, with a sole exception found in Glyptodons, a giant-sized fossil clade, for which the results were consistent with directional selection (Machado et al., 2022). Collectively, these findings suggest that the signal of directional selection is not uniformly erased at macroevolutionary scales, but rather that its detectability varies across clades, traits, and evolutionary contexts.

Here, we revisit the long-standing view that peak dynamics dominate large-scale phenotypic evolution, progressively obscuring the signal of directional selection over macroevolutionary timescales (Hansen, 1997; Lynch, 1990; Uyeda et al., 2011). Specifically, we test whether directional selection remains detectable using standard quantitative-genetic methods across mammalian transitions into new adaptive zones. We focus on the mammalian skull because this structure is a semi-autonomous morphological system, highly informative about species' ecologies, and therefore a likely target of natural selection (Machado, 2020; Marroig & Cheverud, 2004; Roseman, 2004). Adaptive zone transitions are particularly suitable for this test because they are expected to involve prolonged and intense periods of directional selection as lineages invade novel ecological regimes (Machado et al., 2022; Rossoni et al., 2017; Schroeder & von Cramon-Taubadel, 2017). By explicitly bracketing evolutionary transitions, we anticipate that we can diagnose events that required stronger directional selection, potentially leaving a significant signal even in comparative data.

Materials and methods

Adaptive zone transitions

For more than 75 years, Simpson's concept of "adaptive zones" has played a crucial role in our understanding of the evolutionary process over long timescales (Simpson, 1944, 1953). Under this model, an adaptive zone is a restricted region of the phenotypic space occupied by species with relatively similar form-function-fitness relationships (Polly, 2008; Simpson, 1953; Van Valen, 1971). Within-zone evolution is usually small in scale and does not involve major ecological changes. Evolution within a zone is thought to happen at exceptionally slow rates (i.e., bradytelic in Simpson's terms), with lineages slowly following adaptive peaks within a restricted region of the morphospace. However, when opportunities arise (e.g., due to the invasion of new environments or extinction of competitors), lineages may experience faster rates of evolution (i.e., tachytelic) while invading new regions of the morphospace, leading to extreme evolutionary change associated with shifts in ecology and in the structure and distribution of adaptive peaks (Simpson, 1944, 1953; Uyeda et al., 2011).

Here, we applied the concept of adaptive zones to diagnose and define evolutionary transitions worth investigating. Because invasions of new adaptive zones are marked by increased rates of evolution, they are more likely to retain the signal of directional selection, even over longer timescales. Specifically, we use Polly (2008)'s formalization, which suggests that a phenotype is considered to inhabit a new adaptive zone if it (a) evolved later; (b) presents new ecological features; and (c) falls outside the distribution of phenotypes that belong to the ancestral adaptive zone. To achieve this, within each clade, we classified species into two major ecological groups: one belonging to an ancestral group and the other to a recently evolved one. Species were assigned to a new adaptive zone if they differed in dietary or locomotory ecology and were considered morphologically disjunct from the ancestral zone (see Appendix for more details).

Two general categories can be used to describe the relationship between adaptive zones in each transition. The first (henceforth, the "nested" type) corresponds to arrangements where lineages associated with the new adaptive zone are nested within a more inclusive clade of species belonging to the ancestral zone (e.g., Glyptodonts are nested within armadillos, therefore evolving from an armadillo-like ancestor; Figure 1A; Machado et al., 2022). In this case, we have direct access to phenotypes that represent the ancestral adaptive zone. The second category (the "analog" type) is based on identifying an extant analog for an extinct grade of species that preceded the invasion of the new adaptive zone [e.g., saber-toothed cats evolved from the *Pseudaelurus* grade of conical-shaped cats, functionally similar to Pantheridae; Figure 1B; (Simpson, 1944)]. Using these analogs is essential because, in these cases, we did not have access to a direct representative of the potential ancestral morphologies.

Downloaded from academic.oup.com/evlett/advance-article/doi/10.1093/evlett/qrag039/8863744 by Maria Mestriner user on 30 October 2026

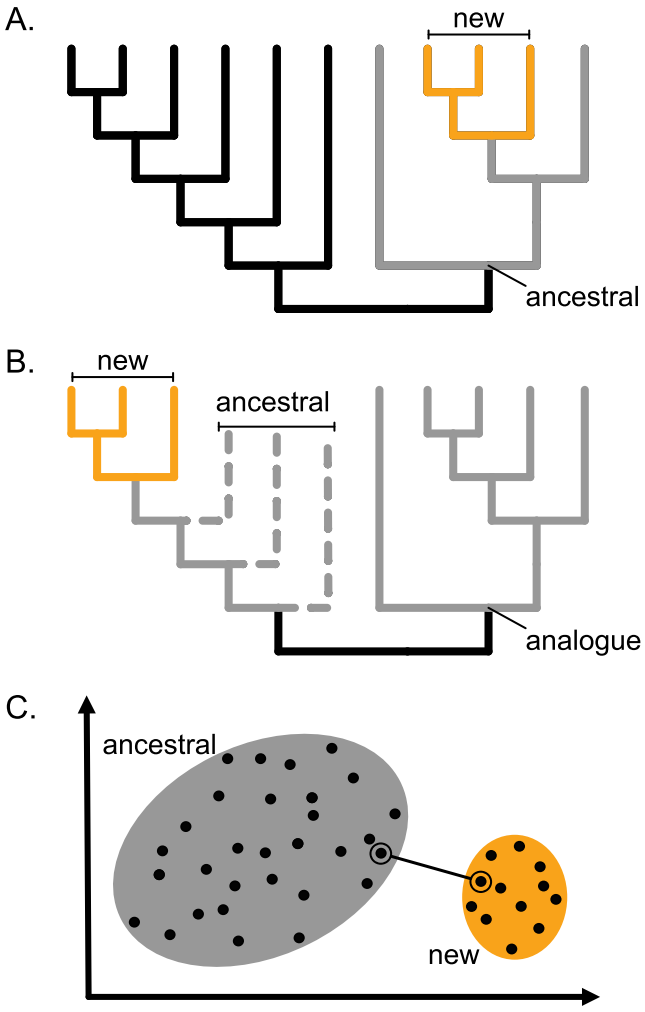


Figure 1. Examples of nested (A) and analog (B) adaptive zone transitions. Gray lineages are under the ancestral adaptive zone (or its analog), and orange lineages are under the new adaptive zone. Dotted lines represent extinct lineages. Ellipses on the hypothetical morphospace (C) represent both adaptive zones. The solid line connects the closest neighboring species used to model the transition among zones.

To model the invasion of a new adaptive zone, we identified, for each clade, the shortest distance between sampled phenotypes that leads to a transition between the ancestral and the new adaptive zone (Figure 1C, see below). The starting species is defined as the member of the ancestral adaptive zone that is morphologically closest to a member of the new zone, while the end species is the member of the new adaptive zone that is closest to the starting species. Even though these species are relatively close in morphospace, they are generally not the closest phylogenetic relatives, as many modeled transitions involve different genera (Table 1). These species are therefore not interpreted as literal ancestors and descendants. Rather, they define a minimum phenotypic displacement required to move between adaptive zones.

We focused on 12 mammalian clades that exhibit between-lineage transitions consistent with the definition of adaptive-zone shifts used here (Table 1). These transitions were selected because the derived lineages differ from their putative ancestral

Table 1. Adaptive zone transitions examined. **Clade**- Focal clades of analyses used to define ancestral adaptive zones. **New zone**- taxa thought to have colonized a new adaptive zone, **Species**- number of species in the ancestral zone and in the new zone, respectively. **Type**- Type of adaptive zone transition modeled. See text and Figure 1A, B for full description. **Start** and **End**- Species chosen for the start and end of the adaptive zone transition. Numbers in parentheses are sample sizes. **Time** (myr) - Time in million years estimated for the transition according to phylogenetic and paleontological information. $\mathbf{gen_t}$(y) - Mean and standard deviation for the generation time in years for each clade. Sample details for $\mathbf{gen_t}$(y) can be found in Kuderna et al. (2023).

Clade	New Zone	Species	Type	Start	End	Time (myr)	$\mathbf{gen_t}$(y)
Didelphimorphia	Didelphini	21/10	Nested	*Marmosa demerarae* (168)	*Caluromys philander* (135)	5.00	1.92 (0.36)
Cingulata	Glyptodontinae	12/5	Nested	*Euphractus sexcinctus*(128)	*Glyptotherium* (1)	3.00	5.10 (2.31)
Canidae	*Speothos*	10/1	Nested	*Cerdocyon thous* (76)	*Speothos venaticus* (56)	2.70	4.50 (0.72)
Ursidae	*U. maritimus*	2/1	Nested	*Ursus arctos* (67)	*Ursus maritimus* (83)	0.50	14.77 (1.71)
Pinnipedia	Odobenidae	13/1	Analog	*Otaria byronia* (25)	*Odobenus rosmarus* (34)	1.50	11.20 (2.02)
Felidae	Machairodontinae	7/1	Analog	*Panthera leo* (50)	*Smilodon populator* (1)	3.20	7.91 (1.32)
Mormoopidae	*Mormoops*	15/2	Analog	*Pteronotus fulvus* (172)	*Mormoops blainvillei* (63)	2.71	5.42 (0.27)
Phyllostomidae	Stenodermatinae	14/8	Nested	*Sturnira lilium* (31)	*Pygoderma bilabiatum* (55)	4.70	5.59 (0.15)
Oryzomyini	*Holochilus*	22/2	Nested	*Sooretamys angouya* (25)	*Holochilus brasiliensis* (42)	1.33	1.65 (0.25)
Cheirogalidae	*Microcebus*	8/6	Nested	*Cheirogaleus medius* (34)	*Allocebus trichotis* (1)	1.30	5.75 (0.50)
Ceboidea	Callitrichidae	18/33	Nested	*Saimiri vanzolinii* (14)	*Leontopithecus rosalia* (36)	3.03	7.81 (3.23)
Hominidae	*Homo*	5/1	Nested	*Pan troglodytes* (91)	*Homo sapiens* (237)	6.60	21.39 (2.19)
Total		218					

Downloaded from academic.oup.com/evlett/advance-article/doi/10.1093/evlett/qrag039/8863744 by Maria Mestriner user on 30 October 2026

zones not only in skull morphology, but also in ecological or functional attributes described independently of the present analyses. In Didelphimorphia, we examined the emergence of large-bodied South American opossums (Didelphini) from smaller didelphid ancestors. In Cingulata, we assessed the evolution of herbivorous, heavily armored glyptodonts (Glyptodontinae) from armadillo-like ancestors. In Canidae, we analyzed the evolution of the hypercarnivorous bush dog (*Speothos venaticus*) relative to more generalized South American canids. In Ursidae, we studied the divergence of the marine-specialized and hypercarnivorous polar bear (*Ursus maritimus*) from more generalist bears such as *U. arctos* and *U. americanus*. In Pinnipedia, we focused on the origin of mollusk-feeding walruses (Odobenidae) from more generalized otariid-like ancestors. In Felidae, we evaluated the shift from conical-toothed, panther-like felids to saber-toothed cats (Machairodontinae). In Mormoopidae, we examined the evolution of ghost-faced bats (*Mormoops*), which show distinctive craniofacial morphology and dietary specialization relative to more generalized insectivorous *Pteronotus*. In Phyllostomidae, we considered the emergence of specialized fruit-eating Stenodermatinae from insectivore-frugivore ancestors. In Oryzomyini, we traced the adaptation of *Holochilus* to semiaquatic habitats from terrestrial oryzomyine ancestors. Among primates, we focused on two independent cases of miniaturization: the evolution of mouse lemurs (*Microcebus*) within Cheirogaleidae and the evolution of marmosets and tamarins (Callitrichidae) within Ceboidea. We also examined the divergence of humans (*Homo sapiens*) from other apes within Hominidae, a transition associated with substantial craniofacial reorganization. A more thorough description, justification, and references for these transitions are provided in the Appendix. From this point forward, we refer to each transition by the most inclusive taxon named above, and to the new adaptive zone by the less inclusive taxon (Table 1).

For the timing of each transition, we used information from phylogenetics and the fossil record to bracket the specific period of the invasion. For nested adaptive zones, this bracket typically lies between the origin of the first lineage in the new zone and the divergence time of a sister lineage still within the ancestral one. For the extant analog case, we used fossil-record data to bracket the origins of the last species in the ancestral grade and the first species in the new clade. See Appendix for specific information on each transition.

Sample and morphometrics

We evaluated the morphology of 231 species, comprising a total of 11,793 specimens (Table 1). Samples were obtained from 43 museums distributed worldwide (see acknowledgments). We primarily targeted adult specimens to minimize potential bias in estimating covariances arising from grouping across ontogenetic stages (Hubbe et al., 2023). Maturity was inferred based on complete dental eruption, fusion of the basicranial sutures, and overall morphology consistent with that of adults in each species (Hubbe et al., 2016; Machado et al., 2018). For Rodentia and Didelphimorphia, adult age classes were determined using dental age categories based on tooth eruption and wear (Hubbe et al., 2023). The age factor was statistically controlled for in these groups (see below). For Carnivora, we also included subadult specimens (skull size and shape consistent with adult morphology but without complete fusion of basicranial sutures), as their cranial measurements showed no significant differences from those of adults (Machado et al., 2018).

To quantify skull morphology, we calculated 33 standardized linear distances from 32 homologous anatomical landmarks, as described in Machado et al. (Machado et al., 2022). Landmarks were obtained using a Microscribe digitizer for most of our sample (de Oliveira et al., 2009; Hubbe et al., 2016; Machado et al., 2018; Pavan & Marroig, 2016; Porto et al., 2009; Rossoni et al., 2019), while the New World Monkey dataset was digitized with a Polhemus 3Draw digitizer (Marroig & Cheverud, 2001). Bilaterally symmetrical measurements were averaged within a specimen. Traits were set on the ratio (proportional) scale through log-transformation (Houle et al., 2011; Voje et al., 2023) following Holstad et al. (2024). To visually inspect species distribution across morphospaces, we performed principal component analysis (PCA) of the between-species covariance matrix.

For each species in our sample, we obtained a vector of average measurements, and the pairwise Euclidean distances between species in each clade were calculated. The shortest distance between species averages belonging to different adaptive zones was recorded as the distance needed for that transition, and the end-point species were selected for further analyses (Figure 1C, Table 1). Using other metrics (e.g., Mahalanobis distance) didn't change our overall results.

Rate test

To test whether adaptive-zone transitions retain a detectable signal of directional selection, we quantified the rate of multivariate phenotypic change required to cross the inferred gaps between adaptive zones. We used a quantitative-genetic test based on the Lande Generalized Genetic Distance (LGGD) (Lande, 1979), calculated as:

$$LGGD = \frac{N_e}{t}\Delta z^t \mathbf{G}^{-1}\Delta z \quad (1)$$

where t is the time of divergence in generations, N_e is the effective population size, Δz is a vector representing the evolutionary transition for each trait, and $\mathbf{G}$ is the matrix of additive genetic variance and covariance among traits. The LGGD is thus a rate version of the Mahalanobis distance that uses quantitative genetics parameters to scale multivariate phenotypic change among lineages in units of standing genetic variation. So two transitions with the same phenotypic distance can have very different LGGD values if one occurred over a much shorter timescale or involved traits with less genetic variance available for evolution.

Solely under genetic drift, evolutionary change is expected to accumulate according to Lande's equation of multivariate genetic drift (Lande, 1979):

$$\mathbf{B} = \frac{t}{N_e}\mathbf{G} \quad (2)$$

where $\mathbf{B}$ is the covariance matrix between evolutionary changes. This equation provides the null expectation against which we compared our observed distribution of LGGD. We used this method instead of expectations generated by parametric methods because the latter produce inadequate type-I error rates (Machado et al., 2022). In empirical applications, LGGD values that fall within the simulated drift interval can be interpreted as consistent with neutral genetic drift, whereas values that deviate substantially above or below this range indicate evolutionary rates more compatible

Downloaded from academic.oup.com/evlett/advance-article/doi/10.1093/evlett/qrag039/8863744 by Maria Mestriner user on 30 October 2026

with directional or stabilizing selection, respectively. These are the direct interpretations of the statistic, but LGGD is ultimately a summary measure of phenotypic divergence over an entire time interval. As a result, heterogeneity in the underlying evolutionary process can affect its value. For instance, values below the drift expectation may arise from prolonged periods of stasis following initial episodes of directional selection (Machado et al., 2022). Consequently, LGGD should be interpreted as an average signal of evolutionary dynamics across the divergence period, rather than as a complete description of the sequence of processes that occurred during that interval.

These methods depend on estimating **G**, which requires data from a population with known genetic relatedness (Falconer & Mackay 1996). Because our samples come from museum collections with unknown relationships, we rely instead on the observation that phenotypic correlations—i.e., the sample correlation among traits—are a good approximation of the underlying genetic correlations (Cheverud, 1988), a fact thoroughly validated for mammalian skulls (Garcia et al., 2014; Hubbe et al., 2023; Marroig & Cheverud, 2010; Porto et al., 2009, 2015). Furthermore, phenotypic variance has been shown to scale linearly with additive genetic variance (Holstad et al., 2024). Together, these suggest that we can model **G** using phenotypic correlations and variances, i.e., the phenotypic covariance matrix **P**.

We calculated **P** for each of the starting species (Table 1) by removing confounding effects (e.g., age, sex, geography) using a linear model approach (Marroig & Cheverud, 2001). Using different **P** matrices from other species within the same clade or pooled within-group matrices did not alter our results, in line with evidence showing that such matrices are stable within mammalian orders (de Oliveira et al., 2009; Marroig & Cheverud, 2001; Machado et al., 2018; Hubbe et al., 2016; Rossoni et al., 2019). We therefore present only the results based on the starting-species matrix for simplicity.

To address estimation uncertainty, we employed a Bayesian approach with a weak uninformative Wishart prior (Melo et al., 2015), drawing 1000 samples from the posterior distribution of Ps for each analysis. The use of uninformative priors has a similar effect as a shrinkage operation, which has been shown to reduce noise in the estimation of covariance matrices (Marroig et al., 2012). We then modeled **G** as

$$\mathbf{G} = \mathbf{H}\mathbf{P}_\mathbf{w}\mathbf{H} \tag{3}$$

with **H** being a diagonal matrix with the square root of each trait's h^2 along the diagonal. This transformation assumes that phenotypic correlations approximate genetic correlations, while allowing the total amount of additive genetic variation to vary across traits and heritabilities. For h^2, we drew values from a uniform distribution ranging from $h^2 = .3 - .6$, which is the range of values for the cranial traits explored here (Garcia et al., 2014; Marroig & Cheverud, 2010; Porto et al., 2009, 2015). The resulting distribution of *G*s thus incorporates uncertainty in the estimate of genetic correlations (approximated by their phenotypic counterparts), phenotypic variances, and heritabilities.

To calculate the morphological change Δz associated with each evolutionary transition, we obtained a posterior distribution of the averages for the start and end species. Posterior parameters were obtained using a conjugate prior and drawing 1000 samples for each trait from the posterior distributions. Differences between posterior samples of the averages were then used to calculate 1000 Δzs.

For t, we divided the divergence time available for each transition by the generation time (gen_t). Clade-wise averages and standard deviations of gen_t were obtained from Pacifici et al. (2013). We used these parameters to generate 1000 gen_t values using a normal distribution. For N_e, we sampled 1000 values from a log-normal distribution with a mean of 11 and standard deviation of 1. The resulting N_e values ranged from 1,000–300,000, consistent with genomic estimates for multiple mammalian species (Brevet & Lartillot, 2021; Kuderna et al., 2023; Lorenzen et al., 2011; Wilder et al., 2023). Lastly, we plotted estimated LGGD against transition times to assess potential time dependence in the estimated rates.

Results

As expected, across most focal clades, species assigned to new adaptive zones occupied regions of the morphospaces that were discontinuous from, or peripheral to, those occupied by species within the ancestral adaptive zones (Figure 2). The degree of separation, however, varied substantially among clades. Some transitions showed clear phenotypic discontinuities between ancestral and derived zones, including Glyptodontinae, Odobenidae, Machairodontinae, Mormoopidae, Ceboidea, and Hominidae (Figure 2). In these cases, the modeled transition crossed an evident gap between the two regions of morphospace. Other transitions were less sharply separated. Didelphimorphia, Oryzomyini, and Phyllostomidae showed new adaptive zones that extended from, or lay close to the edge of, the ancestral distribution (Figure 2), suggesting weaker phenotypic discontinuity between zones. Ursidae represents an ambiguous case: within-zone distances among the sampled bears are greater than the modeled between-zone distance involving polar bears. Because only three species were included, it is unclear whether the zones are adjacent or discontinuous.

Ceboidea presents an interesting case in which the mere identification of discontinuities is not sufficient to establish an adaptive zone transition. While there is a difference between non-miniaturized groups (Cebinae, group PC1 >0) and miniaturized ones (Callitrichidae, PC1 <0), one could argue that differences within zones are larger than between zones. This is highlighted by the close proximity of most Callitrichidae and squirrel monkeys (*Saimiri*) near the origin of the plot, as well as by the extremes of the first PC axis, with *Callithrix pigmaea* showing extreme negative PC1 values and the *Sapajus* genus displaying extreme positive values. While it would be tempting to group squirrel monkeys within the miniaturized zone, this group lacks other life-history and morphological adaptations thought to be associated with miniaturization, as observed in Callitrichidae (Ford, 1980; Harris et al., 2014; Martin, 1992; Montgomery & Mundy, 2013). Similarly, while *Callithrix pigmaea* is morphologically extreme within the Callitrichidae (Ford, 1980), it does share similar traits with the rest of the miniaturized clade.

The LGGD simulations under genetic drift produced lower and upper bounds of approximately 19 and 50 LGGD units ($D^2 N_e t^{-1}$), respectively (Figure 3). Most modeled adaptive-zone transitions exceeded this interval, consistent with rates higher than expected under drift. The strongest signals were observed for Odobenidae

Downloaded from academic.oup.com/evlett/advance-article/doi/10.1093/evlett/qrag039/8863744 by Maria Mestriner user on 30 October 2026

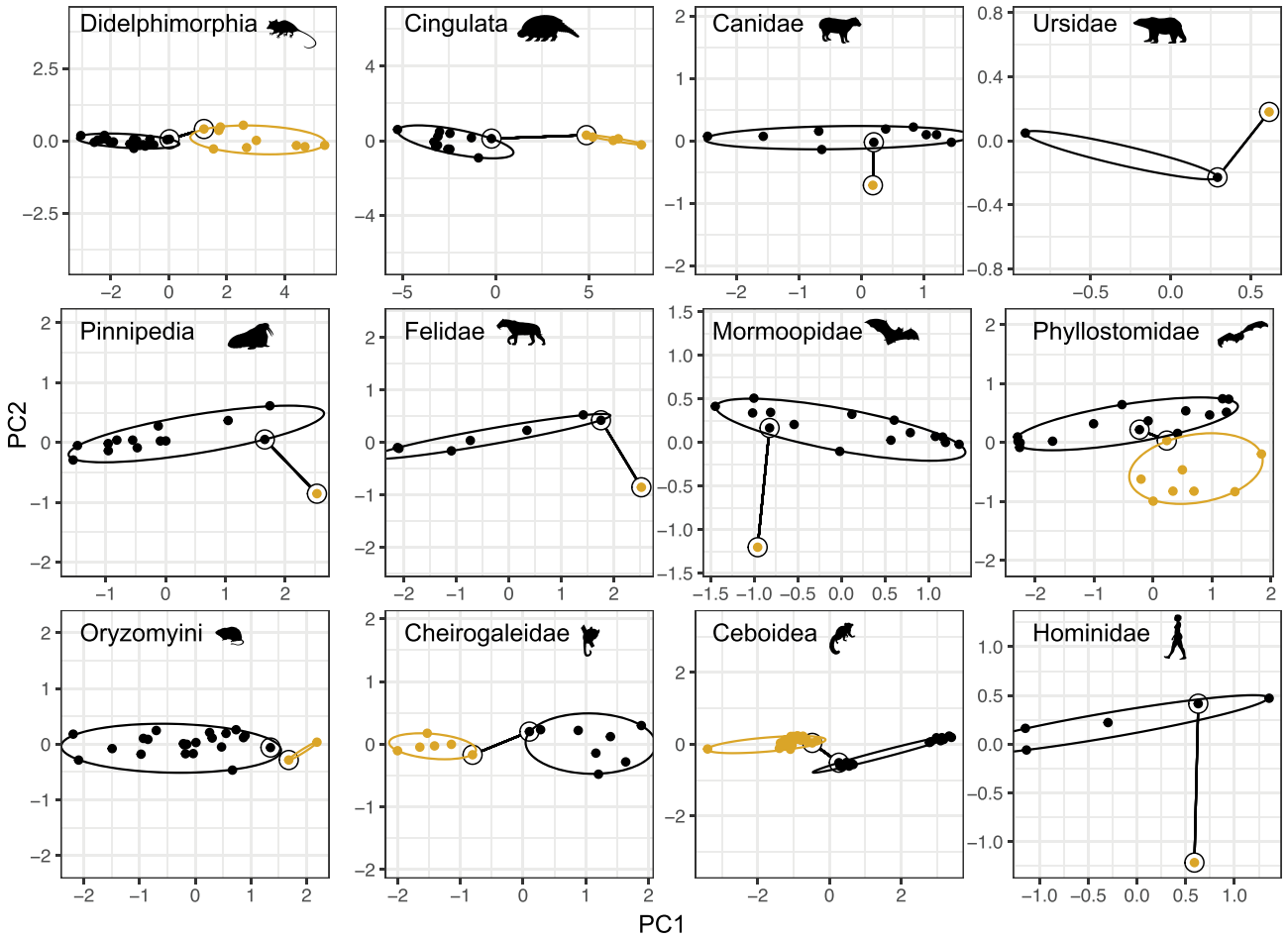


Figure 2. Distribution of the first two principal components of species averages for each focal clade. Species from the ancestral adaptive zone are represented in black, and the new adaptive zone is represented in gold. Curved solid lines represent the ellipsoidal envelope containing all species from a respective adaptive zone. Solid lines connect the pair of extreme species for each transition. Panels are in different scales. Silhouettes were obtained from https://www.phylopic.org/ under Creative Commons licenses (CC0 1.0, CC BY 3.0)

and Glyptodontinae, whose LGGD distributions were clearly above the drift expectation. Several other transitions, including Felidae, Mormoopidae, Phyllostomidae, Ursidae, Ceboidea, and Hominidae, had median values, and often interquantile ranges above the upper boundary expected for drift, although the magnitude varied among clades.

A smaller set of transitions showed weaker or no evidence of rates above drift expectations. Cheirogalidae and Canidae had median LGGD values near the upper bounds for drift, while Didelphimorphia and Oryzomyini values fell below the expected interval for drift. The low LGGD values observed for the two latter groups also correspond to the weaker visual separation observed in the morphospace, particularly for Oryzomyini, in which the new adaptive zone lies near the edge of the ancestral distribution (Figure 2).

Contrary to the expectation that evolutionary rates tend to decline with increasing temporal interval, we found no consistent relationship between LGGD and time intervals (Figure 4). Pearson correlation coefficients calculated between each posterior LGGD sample and divergence time spanned both positive and negative values ($\rho = -0.39$ to 0.41), suggesting that longer transitions were not associated with lower rates of evolution or with a more muted signal of selection.

Discussion

By focusing on evolutionary transitions more likely to involve intense directional selection, we recover here a pattern that contrasts with prevailing expectations from macroevolutionary theory. Evolutionary rates do not appear to decline with time (Figure 4), nor were they constrained below the expectation under drift. Instead, most transitions exhibited rates at or above drift expectations (Figure 3) despite spanning divergence timescales of 0.5–6.6 Myr (Table 1). These results suggest that the apparent "disappearance" of signals of directional selection at macroevolutionary scales might not be an inevitable consequence of temporal averaging. Rather, when we examine evolutionary change within biologically meaningful time intervals that bracket adaptive transitions, the signals of directional selection can remain detectable even over millions of years. More broadly, our findings support the idea that adaptive-zone invasions represent a class of evolutionary events in which adaptation and directional selection can leave persistent signals at macroevolutionary scales.

Among all tested transitions, those with the strongest signal of directional selection were walruses and glyptodonts. One possible explanation for this might be the direction of divergence

Downloaded from academic.oup.com/evlett/advance-article/doi/10.1093/evlett/qrag039/8863744 by Maria Mestriner user on 30 October 2026

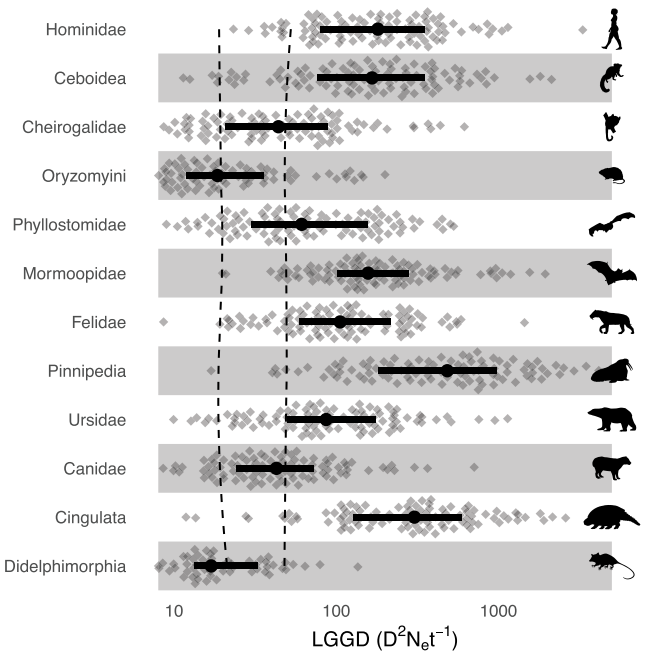


Figure 3. LGGD values for each adaptive zone transition. Diamonds represent each individual value of LGGD, dots are the medians and solid horizontal lines represent the interquantile ranges. Dashed vertical lines traversing all panels represent the lower and upper rates expected under drift estimated by simulation.

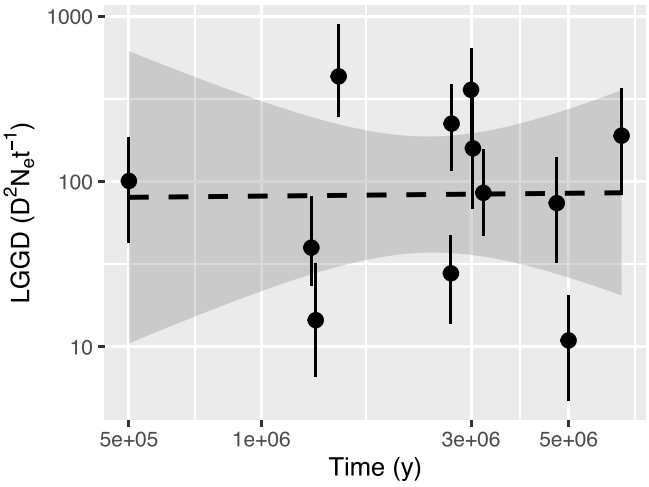


Figure 4. Relationship between rates of evolution, as measured by LGGD, and the timing of adaptive-zone transitions.

between ancestral and new adaptive zones in these transitions. Both glyptodonts and walruses have skulls that are dorsoventrally expanded relative to their sister taxa (a phenomenon described for glyptodonts as "telescoping"; Farina & Vizcaíno, 2001). In mammals, size is typically the major axis of variation (Marroig & Cheverud, 2005), and thus the main direction of evolutionary potential (evolvability; Hansen & Houle, 2008), closely followed by independent changes in the relative size of the neurocranium and facial regions (Machado et al., 2018; Marroig & Cheverud, 2010; Rossoni et al., 2024). Because, all being equal, higher evolvabilities along directions of selection decrease LGGD estimates (equation 1), this might explain why adaptations along either size (e.g., Ceboidea, Cheirogalidae) or craniofacial length adjustments (e.g., Canidae, Ursidae, Phyllostomidae) registered relatively lower LGGD values. However, since the evolution of walruses and glyptodonts might involve variation along directions of lower evolvability, greater intensity of selection might have been necessary to overcome the relative constraints imposed by patterns of trait covariation (Marroig & Cheverud, 2005; Machado, 2020). These results suggest that the detectability of directional selection may depend on both the magnitude of ecological and morphological change and the alignment between evolutionary trajectories and the structure of available phenotypic variation.

The only clades falling below the expectation under drift are Didelphimorphia and Oryzomyini, which likely reflect clade-specific contingencies. In marsupials, size variation dominates evolutionary potential, facilitating adaptation along this dimension (Lemos et al., 2001; Porto et al., 2015). For rodents, however, the presence of a highly versatile skull morphology (Maestri et al., 2017) might reduce the selective intensity required for eco-morphological change (Machado, 2020). Similar factors may account for the lower LGGD observed in Cheirogalidae and Canidae. For Cheirogalidae, differentiation between the new and ancestral zones occurred primarily along the size dimension, a well-known line of least resistance in primates (Marroig & Cheverud, 2005, 2010). On the other hand, while the selection pressure for a hypercarnivore diet in Canidae was mainly focused on reducing facial length to improve bite force (Machado, 2020), the facial region in this clade seems to have greater evolutionary flexibility (Machado et al., 2018, 2019), which might have increased evolutionary potential in the direction of selection, thus decreasing LGGD estimates.

Among bats, both groups showed rates above those expected under drift, with Phyllostomidae presenting lower values than Mormoopidae. This is a surprising result, since the former is routinely considered a classic example of adaptive radiation (Rossoni et al., 2017). Differences among groups, however, might relate to the same processes that led to the divergence of walruses and glyptodonts. The skull morphology of Stenodermatinae (obligate frugivore bats) is marked by an extreme reduction in facial length, which might have been facilitated by a more modular skull observed in Phyllostomids (Rossoni et al., 2024). Although a direct investigation of Mormoopidae skull modularity has not been conducted, it is unlikely that this group differs radically from established patterns for mammals or Chiroptera (Porto et al., 2009; Rossoni et al., 2019). In that case, the extreme inflection observed in the genus *Mormoops* is unlikely to align with any genetic line of least resistance, suggesting that it requires even greater selective pressure. The differences in the signal of selection among bat families further highlight the importance of context, rather than just morphological disparity and ecological shifts, in shaping selective dynamics (Schluter, 2024). In other words, ecological opportunity alone is insufficient to predict evolutionary rates. Instead, the interaction between ecological shifts and the structure of phenotypic integration may be crucial to determining the strength of directional selection required to reach a novel adaptive zone (Machado, 2020).

The results presented here are, of course, contingent on our modeling choices and the assumptions they entail. Some choices

Downloaded from academic.oup.com/evlett/advance-article/doi/10.1093/evlett/qrag039/8863744 by Maria Mestriner user on 30 October 2026

could inflate or underestimate the magnitude of the inferred rates, but most are unlikely to alter the central conclusion that adaptive-zone transitions often exceed drift expectations. For example, by defining adaptive zones from observed phenotypes, we necessarily treat sampled species as proxies for broader form-function-fitness relationships. Incomplete sampling, especially of fossil or unsampled extant intermediate forms, could therefore inflate distances between adaptive zones and, consequently, the inferred evolutionary rates. On the other hand, models of evolution that include pleiotropic effects on additional traits generally predict slower evolutionary responses than models that account only for focal traits (Hansen & Houle, 2008; Jiang & Zhang, 2020; Jiang & Pennell, 2025), implying that our estimates of the selection signal are in fact conservative, as they may underestimate the strength of selection required to produce the observed transitions. Therefore, while the exact magnitude of the inferred rates remains sensitive to modeling choices, the presence of elevated evolutionary rates across most adaptive-zone transitions appears robust to reasonable biological assumptions.

More caution may be warranted in our interpretation of transitions for which the new zone lies close to the edge of the ancestral distribution, such as in Didelphimorphia and Oryzomyini. Because both groups exhibit highly conserved and presumably versatile cranial morphologies, assigning specific taxa to different adaptive zones may not be justified. In those cases, the lower rates of evolution found here could, in fact, be representative of within-zone bradytelic evolution (Simpson, 1944). By contrast, transitions such as Glyptodontinae, Odobenidae, Machairodontinae, and Hominidae involve clearer ecological and morphological discontinuities and are less likely to be explained solely by incomplete sampling of intermediate phenotypes. These cases, therefore, provide stronger evidence that adaptive-zone transitions can retain a detectable signal of directional selection.

Finally, this study is not intended as a methodological template for estimating the strength of selection during adaptive-zone transitions. Our goal is more limited: to test whether directional selection can leave detectable signatures in macroevolutionary data when transitions are defined and temporally bracketed using independent comparative, phylogenetic, and paleontological information. We therefore selected cases that were especially likely to involve sustained adaptation into new adaptive zones. As a result, our findings show that such signals can persist under favorable conditions, but they should not be used to infer how frequently directional selection remains detectable across macroevolutionary datasets more generally.

We note, however, that previous studies using comparative quantitative-genetic frameworks have reached similar conclusions (Latrille et al., 2024; Machado et al., 2022, 2023; Schroeder et al., 2014; Schroeder & Ackermann, 2017). Together with these studies, our results challenge the assumption that directional selection is necessarily obscured at macroevolutionary timescales. They instead suggest that adaptive-zone transitions may provide especially favorable contexts for detecting how microevolutionary processes contribute to large-scale phenotypic diversification.

Future work should move beyond asking whether signals of directional selection can persist and instead test how often, and under what ecological contexts, they shape the tempo of evolution. Achieving this will require models of phenotypic evolution that more fully integrate comparative phylogenetic methods, quantitative-genetic frameworks, and fossil data.

Data and code availability

Necessary data and code to replicate all analyses are available at https://github.com/MachadoFA/AdapZones.

Author contributions

F.A.M. and A.H. developed the research question. A.H. collected data on Cingulata. B.A.C. collected data on rodents. F.A.M. and T.M.G.Z. collected data on carnivores. G.M. and A.P. collected data on primates. A.C.P. and D.M.R. collected data on bats. A.P. and H.S. collected data on Didelphidae. F.A.M. and D.M. developed the analytical and computational analyses. F.A.M. wrote the first draft, and all authors contributed to later drafts and discussion.

Funding

This work was supported by Fundanção de Amparo a Pesquisa do Estado de São Paulo (FAPESP, grant numbers: GM- 2009/05687-9, 2011/14295-7; FAM - 2011/21674-4, 2013/22042-7; AH- 2011/14295-7, 2012/24937-9, 2014/26262-4; BAC- 2009/51825-4, 2015/16598-8; TMGZ- 2013/07299-1, 2014/12403-5; AP- 2013/06577-8 and 2014/15116-7; ACP- 2009/54731-0, 2011/14295-7; DMR- 2009/50378-4, 2014/12632-4; HS- 2006/53774-0, 2010/12810-9).

F.A.M. was partially supported by the Department of Biology of Oklahoma State University. A.P. was supported in part by the U.S. National Science Foundation under Award No. 2422839. Any opinions, findings, conclusions, or recommendations expressed in this material are those of the authors and do not necessarily reflect the views of the National Science Foundation.

Conflict of interest

All authors declare no conflict of interest.

Acknowledgments

We thank the curatorial staff of the following institutions for allowing access to their collection: American Museum of Natural History (AMNH), British Museum of Natural History (BMNH), *Coleção de Chiroptera de São José do Rio Preto* (DZSJRP), Duke Primate Center (DUPC), *Facultad de Ciencias Naturales y Museo de La Plata* (FCNyM), Field Museum (FMNH), *Faculdad de Ciencias de la Universidad de la Republica* (FC-UDELAR), Florida Museum of Natural History (UF), *Instituto de Pesquisas Amazonicas* (INPA), *Instituto de Pesquisas Científicas e Tecnológicas do Estado do Amapá* (IEPA), Kentucky University (KU), Los Angeles County Museum (LACM), *Naturhistorisches Museum, Wien* (NMW), *Museo Argentino de Ciencias Naturales "Bernardino Rivadavia"* (MACN), *Museo de Historia Natural de la Universidad Nacional Mayor de San Marcos* (MUSM), *Museo Municipal de Colonia* (MMC), *Museo Nacional de Historia Natural* (MNHN-UY), *Museu de Anatomia Humana da Uni-*

Downloaded from academic.oup.com/evlett/advance-article/doi/10.1093/evlett/qrag039/8863744 by Maria Mestriner user on 30 October 2026

versidade Federal de São Paulo (MAH-UNIFESP), *Museu de Anatomia Humana Professor Alfonso Bovero* (MAHPAB), *Museu de Ciências Naturais da Fundação Zoobotânica do Rio Grande do Sul* (MCNRGS), *Museu de Ciências Naturais da PUC-MINAS* (MCN), *Museu de Zoologia da Universidade de São Paulo* (MZUSP), *Museu Nacional do Rio de Janeiro* (MNRJ), *Museu Paraense Emílio Goeldi* (MPEG), *Museum d'Histoire Naturelle, Geneve* (MHNG), *Museum für Naturkunde* (MfN, ZMB), *Muséum National d'Histoire Naturelle* (MNHN-FR), Museum of Comparative Zoology (MCZ), Museum of Vertebrate Zoology (MVZ), *Naturhistorisches Museum, Bern* (NHM), Royal Belgian Institute for the Natural Sciences (RBINS), Royal Museum for Central Africa (RMCA), Royal Ontario Museum (ROM), *Senckenberg Naturmuseum Frankfurt* (SMF), Smithsonian Institute (USNM), Texas Tech University (TTU), *Universidade Federal da Minas Gerais* (UFMG), *Universidade Federal da Paraíba* (UFPB), *Universidade Federal do Pernambuco* (UFPE), *Universidade Federal do Piauí* (UFPI), University Museum of Zoology, Cambridge (UMZC), *Zoologisches Forschungsmuseum Alexander Koenig* (ZFMK). We also acknowledge M. Teixeira, P. Auricchio, and V. Tavares for access to specimens under their care. We thank Josef Uyeda for his insights into a previous version of the manuscript and Leonardo Borges for his assistance with Figure 1.

Appendix A

Justification for transition choices

In Didelphimorphia, we examined the emergence of large-bodied South American opossums in Didelphini from smaller-bodied didelphid ancestors. Larger didelphimorphia experience significantly diverse ecological and biomechanic pressures, leading to more morphological diversification than what is observed in small-bodied species (Astúa, 2009; Amador & Giannini, 2016; Abreu & Astúa, 2025; Silva-Neto et al., 2024).

In Cingulata, we assessed the evolution of Glyptodontinae from armadillo-like ancestors. Glyptodonts represent a distinctive herbivorous, heavily armored radiation within Cingulata, which shows significant functional differences from extant armadillos (Cuadrelli et al., 2020; Machado et al., 2022; Vizcaíno et al., 2011).

Among Carnivora, we investigated four transitions: within Canidae, Ursidae, Pinnipedia and Felidae. In Canidae, we analyzed the evolution of the bush dog *Speothos venaticus*. These South American canids possess multiple cranial and mandibular specializations associated with hypercarnivory, in contrast to the more generalist South American canids (Beisiegel & Zuercher, 2005; Machado, 2020; Perini et al., 2010; Ruiz et al., 2023; Van Valkenburgh, 1991). In Ursidae, we studied the divergence of the polar bear *Ursus maritimus* from more generalist brown and black bears. This transition was accompanied by strong ecological, dietary, and physiological specialization for Arctic environments and marine mammal prey, rather than the more omnivorous diet seen in Ursinae (Liu et al., 2014; Polly, 2024; Slater et al., 2010). In Pinnipedia, we focused on the evolution of walruses (Odobenidae). Walruses have a highly modified tusked skull and engage in suction-feeding, diverging greatly from more primitive members of the group, which were generalized piscivores closely resembling otariids (Boisville et al., 2024; Horikawa, 1994; Hocking et al., 2021; Repenning, 1976). In Felidae, we evaluated the transition from conical-toothed felids to saber-toothed Machairodontinae. Saber-toothed cats are characterized by elongate upper canines, reflecting a disparate strategy for prey dispatching than that seen in conical-toothed felids (Chatar et al., 2022; Emerson & Radinsky, 1980; Martin, 1980; Piras et al., 2018; Tamagnini et al., 2023).

Among bats, we analyzed two groups: Mormoopidae and Phyllostomidae. In Mormoopidae, we examined the evolution of ghost-faced bats *Mormoops*. *Mormoops* exhibits one of the most extreme morphologies in bats, with a pronounced dorsal inflection of the palate, a feature likely associated with a specific echolocation strategy and dietary specialization on lepidopterans (Gilley et al., 2025; Pavan et al., 2019; Rolfe et al., 2014). In Phyllostomidae, we considered the emergence of Stenodermatinae, a diverse radiation of specialized fruit-eating bats whose craniodental morphology is associated with the processing of soft and hard fruits, from insectivore-frugivore ancestors (Dumont et al., 2012; Rossoni et al., 2017).

In Oryzomyini, we traced the evolution of the marsh rats *Holochilus* from terrestrial oryzomyine ancestors. This genus is highly adapted to aquatic habitat use, possessing webbed feet and strong craniodental specializations for plant feeding (Tulli & Carrizo, 2024; Soto et al., 2026).

Among primates, we focused on two independent cases of miniaturization: the evolution of mouse lemurs *Microcebus* within Cheirogaleidae, including the smallest living primate species (Masters et al., 2014; Montgomery & Mundy, 2013); and the evolution of small-bodied callitrichids within Ceboidea, a group whose reduced body size and associated life-history traits distinguish them from other New World monkeys (Ford, 1980; Harris et al., 2014; Martin, 1992; Montgomery & Mundy, 2013). Finally, in Hominidae, we examined the divergence of *Homo sapiens* from other apes, a transition associated with marked craniofacial reorganization and previously inferred directional selection along the *Homo* lineage (Schroeder & von Cramon-Taubadel, 2017; Schroeder & Ackermann, 2017).

Temporal bracketing

For each transition, we used phylogenetic or fossil evidence to bracket the time interval over which the adaptive-zone transition plausibly occurred. For Didelphini, we used the interval between the divergence of Didelphini from the remaining Didelphidae and the divergence of *Metachirus* from the remaining Didelphini (Silva-Neto et al., 2024). For Glyptodontinae, we used the interval between the molecularly estimated split of glyptodonts from other armadillos and the occurrence of early specialized glyptodonts such as *Propalaehoplophorus* (Mitchell et al., 2016; Delsuc et al., 2016; Vizcaíno et al., 2011; Cuadrelli et al., 2020). For *Speothos*, we used the timing of South American canid colonization after the formation of the Isthmus of Panama and the Great American Biotic Interchange (Perini et al., 2010). For *Ursus maritimus*, we used molecular estimates of divergence from brown bears (Hailer et al., 2012; Liu et al., 2014). For Odobenidae, we used the interval between late stem odobenids with generalized feeding morphologies, such as *Pontolis*, and the origin of derived Odobeninae (Boessenecker et al., 2023). For Machairodontinae, we used the interval between the last *Pseudaelurus*-grade conical-toothed felids and the origin of saber-toothed machairodontines (Jiangzuo et al., 2023; Paijmans et al., 2017). For *Mormoops*, we used the interval between the split of *Mormoops* from *Pteronotus* and the oldest fossil mormoopids (Morgan et al., 2019; Pavan & Marroig, 2017). For

Downloaded from academic.oup.com/evlett/advance-article/doi/10.1093/evlett/qrag039/8863744 by Maria Mestriner user on 30 October 2026

Stenodermatinae, we used the interval between the split of Stenodermatinae from the ancestral phyllostomid pool and the origin of crown Stenodermatinae (Rojas et al., 2016). For *Holochilus*, we used the interval between the origin of the ancestral lineage leading to *Holochilus*+*Pseudoryzomys* and the cladogenetic event separating these genera (Percequillo et al., 2021). For *Microcebus*, we used the interval between the origin of *Allocebus* and the emergence of *Microcebus* (Wisniewski et al., 2022). For Callitrichidae, although the split from other extant New World monkeys is older, fossil evidence places taxa such as *Lagonimico* and *Aotus dindensis* near the stem of callitrichine evolution and suggests body sizes compatible with larger-bodied New World monkeys; we therefore used the interval between these fossil stem taxa and the origin of crown Callitrichidae to bracket the invasion of the miniaturized callitrichid adaptive zone (Kay, 1994; Fleagle, 2013; Wisniewski et al., 2022). For *Homo*, we used the divergence time from chimpanzees estimated by Schroeder & von Cramon-Taubadel (2017).

References

Abreu, J. A., & Astúa, D. (2025). Comparative and functional anatomy of masticatory muscles and bite force in opossums (didelphimorphia, didelphidae). *The Anatomical Record, 309*(9), 2346–2367. https://doi.org/10.1002/ar.25675

Amador, L. I., & Giannini, N. P. (2016). Phylogeny and evolution of body mass in didelphid marsupials (marsupialia: Didelphimorphia: Didelphidae). *Organisms Diversity & Evolution*, *16*(3), 641–657. https://doi.org/10.1007/s13127-015-0259-x

Astúa, D. (2009). Evolution of scapula size and shape in didelphid marsupials (didelphimorphia: Didelphidae). *Evolution*, *63*(9), 2438–2456. https://doi.org/10.1111/j.1558-5646.2009.00720.x

Beisiegel, B. d. M., & Zuercher, G. L. (2005). Speothos venaticus. *Mammalian Species*, *2005*(783), 1–6. https://doi.org/10.1644/783.1

Boessenecker, R. W., Poust, A. W., Boessenecker, S. J., & Churchill, M. (2023). Tusked walruses (carnivora: Odobenidae) from the miocene–pliocene purisima formation of santa cruz, california (usa): a new species of the toothless walrus valenictus and the oldest records of odobeninae and odobenini. *Journal of Vertebrate Paleontology*, *43*(3), e2296567. https://doi.org/10.1080/02724634.2023.2296567

Boisville, M., Chatar, N., & Kohno, N. (2024). New species of ontocetus (pinnipedia: Odobenidae) from the lower pleistocene of the north atlantic shows similar feeding adaptation independent to the extant walrus (odobenus rosmarus). *PeerJ*, *12*, e17666. https://doi.org/10.7717/peerj.17666

Brevet, M., & Lartillot, N. (2021). Reconstructing the history of variation in effective population size along phylogenies. *Genome Biology and Evolution*, *13*(8), evab150. https://doi.org/10.1093/gbe/evab150

Chatar, N., Fischer, V., & Tseng, Z. J. (2022). Many-to-one function of cat-like mandibles highlights a continuum of sabre-tooth adaptations. *Proceedings of the Royal Society B: Biological Sciences*, *289*(1988), 20221627. https://doi.org/10.1098/rspb.2022.1627

Cheverud, J. M. (1988). A comparison of genetic and phenotypic correlations. *Evolution*, *42*(5), 958–968. https://doi.org/10.1111/j.1558-5646.1988.tb02514.x

Cuadrelli, F., Zurita, A. E., Toriño, P., Miño-Boilini, Á. R., Perea, D., Luna, C. A., Gillette, D. D., & Medina, O. (2020). A new species of glyptodontine (mammalia, xenarthra, glyptodontidae) from the quaternary of the eastern cordillera, bolivia: phylogeny and palaeobiogeography. *Journal of Systematic Palaeontology*, *18*(18), 1543–1566. https://doi.org/10.1080/14772019.2020.1784300

de Oliveira, F. B., Porto, A., & Marroig, G. (2009). Covariance structure in the skull of catarrhini: a case of pattern stasis and magnitude evolution. *Journal of Human Evolution*, *56*(4), 417–430. https://doi.org/10.1016/j.jhevol.2009.01.010

Delsuc, F., Gibb, G. C., Kuch, M., Billet, G., Hautier, L., Southon, J., Rouillard, J. M., Fernicola, J. C., Vizcaíno, S. F., MacPhee, R. D. E., & Poinar, H. N. (2016). The phylogenetic affinities of the extinct glyptodonts. *Current Biology*, *26*(4), R155–R156. https://doi.org/10.1016/j.cub.2016.01.039

Dumont, E. R., Dávalos, L. M., Goldberg, A., Santana, S. E., Rex, K., & Voigt, C. C. (2012). Morphological innovation, diversification and invasion of a new adaptive zone., *Proceedings of the Royal Society of London. Series B, Biological Sciences*, *279*(1734), 1797–1805.

Dzeverin, I. (2008). The stasis and possible patterns of selection in evolution of a group of related species from the bat genus myotis (chiroptera, vespertilionidae). *Journal of Mammalian Evolution*, *15*(2), 123–142. https://doi.org/10.1007/s10914-007-9071-5

Eldredge, N., & Gould, S. J. (1972). Punctuated equilibria: An alternative to phyletic gradualism. Models in paleobiology. *82*(115), 82–115.

Emerson, S. B., & Radinsky, L. (1980). Functional analysis of sabertooth cranial morphology. *Paleobiology*, *6*(3), 295–312. https://doi.org/10.1017/S0094837300006813

Falconer, D. S., & Mackay, T. F. (1996). *Introduction to quantitative genetics*. Longman Green, Harlow, Essex, UK.

Farina, R. A., & Vizcaíno, S. F. (2001). Carved teeth and strange jaws: how glyptodonts masticated. *Acta Palaeontologica Polonica*, *46*(2), 219–234.

Fleagle, J. (2013). *Primate adaptation and evolution (3rd ed)*. Academic Press/Elsevier, Boston, MA.

Ford, S. M. (1980). Callitrichids as phyletic dwarfs, and the place of the callitrichidae in platyrrhini. *Primates*, *21*(1), 31–43. https://doi.org/10.1007/BF02383822

Garcia, G. R. G., Hingst-Zaher, E., Cerqueira, R., & Marroig, G. (2014). Quantitative genetics and modularity in cranial and mandibular morphology of calomys expulsus. *Evolutionary Biology*, *41*(4), 619–636. https://doi.org/10.1007/s11692-014-9293-4

Gilley, D. T., Santana, S. E., & Arbour, J. H. (2025). Macroevolutionary and biomechanical implications of rostral flexion in bat skulls: a major early driver of cranial evolution in bats. *Biological Journal of the Linnean Society*, *144*(1), blae123. https://doi.org/10.1093/biolinnean/blae123

Gingerich, P. D. (1983). Rates of evolution: effects of time and temporal scaling. *Science*, *222*(4620), 159–161. https://doi.org/10.1126/science.222.4620.159

Gingerich, P. D. (1987). Evolution and the fossil record: patterns, rates, and processes. *Canadian Journal of Zoology*, *65*(5), 1053–1060. https://doi.org/10.1139/z87-169

Gingerich, P. D. (2001). Rates of evolution on the time scale of the evolutionary process. *Genetica*, *112*(1), 127–144. https://doi.org/10.1023/A:1013311015886

Hailer, F., Kutschera, V. E., Hallström, B. M., Klassert, D., Fain, S. R., Leonard, J. A., Arnason, U., & Janke, A. (2012). Nuclear genomic

Downloaded from academic.oup.com/evlett/advance-article/doi/10.1093/evlett/qrag039/8863744 by Maria Mestriner user on 30 October 2026

sequences reveal that polar bears are an old and distinct bear lineage. *Science*, *336*(6079), 344–347. https://doi.org/10.1126/science.1216424

Hansen, T. F. (1997). Stabilizing selection and the comparative analysis of adaptation. *Evolution*, *51*(5), 1341–1351. https://doi.org/10.1111/j.1558-5646.1997.tb01457.x

Hansen, T. F. (2024). Three modes of evolution? remarks on rates of evolution and time scaling. *Journal of Evolutionary Biology*, *37*(12), 1523–1537. https://doi.org/10.1093/jeb/voae071

Hansen, T. F., & Houle, D. (2008). Measuring and comparing evolvability and constraint in multivariate characters. *Journal of Evolutionary Biology*, *21*(5), 1201–1219. https://doi.org/10.1111/j.1420-9101.2008.01573.x

Harris, R. A., Tardif, S. D., Vinar, T., Wildman, D. E., Rutherford, J. N., Rogers, J., Worley, K. C., & Aagaard, K. M. (2014). Evolutionary genetics and implications of small size and twinning in callitrichine primates. *Proceedings of the National Academy of Sciences*, *111*(4), 1467–1472. https://doi.org/10.1073/pnas.1316037111

Hocking, D. P., Park, T., Rule, J. P., & Marx, F. G. (2021). Prey capture and processing in fur seals, sea lions and the walrus, *Ethology and behavioral ecology of otariids and the odobenid*. (pp. 101–121). Springer Cham, Switzerland.https://doi.org/10.1007/978-3-030-59184-7_5

Holstad, A., Voje, K. L., Opedal, Ø. H., Bolstad, G. H., Bourg, S., Hansen, T. F., & Pélabon, C. (2024). Evolvability predicts macroevolution under fluctuating selection. *Science*, *384*(6696), 688–693. https://doi.org/10.1126/science.adi8722

Horikawa, H. (1994). A primitive odobenine walrus of early pliocene age from Japan. *Island Arc*, *3*(4), 309–328. https://doi.org/10.1111/j.1440-1738.1994.tb00118.x

Houle, D., Pélabon, C., Wagner, G. P., & Hansen, T. F. (2011). Measurement and meaning in biology. *The Quarterly Review of Biology*, *86*(1), 3–34. https://doi.org/10.1086/658408

Houle, D., Bolstad, G. H., van der Linde, K., & Hansen, T. F. (2017). Mutation predicts 40 million years of fly wing evolution. *Nature*, *548*(7668), 447–450. https://doi.org/10.1038/nature23473

Hubbe, A., Melo, D., & Marroig, G. (2016). A case study of extant and extinct xenarthra cranium covariance structure: implications and applications to paleontology. *Paleobiology*, *42*(3), 465–488. https://doi.org/10.1017/pab.2015.49

Hubbe, A., Machado, F. A., Melo, D., Garcia, G., Sebastião, H., Porto, A., Cheverud, J., & Marroig, G. (2023). Morphological integration during postnatal ontogeny: implications for evolutionary biology. *Evolution*, *77*(3), 763–775. https://doi.org/10.1093/evolut/qpac052

Jiang, D., & Pennell, M. (2025). Alternative mutational architectures producing identical m-matrices can lead to different patterns of evolutionary divergence. *Genome Biology and Evolution*, *17*(6), evaf099. https://doi.org/10.1093/gbe/evaf099

Jiang, D., & Zhang, J. (2020). Fly wing evolution explained by a neutral model with mutational pleiotropy. *Evolution*, *74*(9), 2158–2167. https://doi.org/10.1111/evo.14076

Jiangzuo, Q., Werdelin, L., Sanisidro, O., Yang, R., Fu, J., Li, S., Wang, S., & Deng, T. (2023). Origin of adaptations to open environments and social behaviour in sabretoothed cats from the northeastern border of the tibetan plateau. *Proceedings of the Royal Society B*, *290*(1997), 20230019. https://doi.org/10.1098/rspb.2023.0019

Kay, R. F. (1994). "Giant" tamarin from the miocene of colombia. *American Journal of Physical Anthropology*, *95*(3), 333–353. https://doi.org/10.1002/ajpa.1330950305

Kuderna, L. F., Gao, H., Janiak, M. C., Kuhlwilm, M., Orkin, J. D., Bataillon, T., Manu, S., Valenzuela, A., Bergman, J., Rousselle, M., Silva, F. E., Agueda, L., Blanc, J., Gut, M., de Vries, D., Goodhead, I., Harris, R. A., Raveendran, M., & Beck, R. M. (2023). A global catalog of whole-genome diversity from 233 primate species. *Science*, *380*(6648), 906–913. https://doi.org/10.1126/science.abn7829

Lande, R. (1979). Quantitative genetic analysis of multivariate evolution, applied to brain: body size allometry. *Evolution*, *33*(1), 402–416. https://doi.org/10.2307/2407630

Lande, R. (1985). Expected time for random genetic drift of a population between stable phenotypic states. *Proceedings of the National Academy of Sciences*, *82*(22), 7641–7645. https://doi.org/10.1073/pnas.82.22.7641

Latrille, T., Bastian, M., Gaboriau, T., & Salamin, N. (2024). Detecting diversifying selection for a trait from within and between-species genotypes and phenotypes. *Journal of Evolutionary Biology*, *37*(12), 1538–1550. https://doi.org/10.1093/jeb/voae084

Lemos, B., Marroig, G., & Cerqueira, R. (2001). Evolutionary rates and stabilizing selection in large-bodied opossum skulls (didelphimorphia: Didelphidae). *Journal of Zoology*, *255*(2), 181–189. https://doi.org/10.1017/S095283690100125X

Liu, S., Lorenzen, E. D., Fumagalli, M., Li, B., Harris, K., Xiong, Z., Zhou, L., Korneliussen, T. S., Somel, M., Babbitt, C., Wray, G., Li, J., He, W., Wang, Z., Fu, W., Xiang, X., Morgan, C. C., Doherty, A., O'Connell, M. J., … Wang, J. (2014). Population genomics reveal recent speciation and rapid evolutionary adaptation in polar bears. *Cell*, *157*(4), 785–794. https://doi.org/10.1016/j.cell.2014.03.054

Lorenzen, E. D., Nogués-Bravo, D., Orlando, L., Weinstock, J., Binladen, J., Marske, K. A., Ugan, A., Borregaard, M. K., Gilbert, M. T. P., Nielsen, R., Ho, S. Y., Goebel, T., Graf, K. E., Byers, D., Stenderup, J. T., Rasmussen, M., Campos, P. F., Leonard, J. A., Koepfli, K.-P., … Willerslev, E. (2011). Species-specific responses of late quaternary megafauna to climate and humans. *Nature*, *479*(7373), 359–364. https://doi.org/10.1038/nature10574

Lynch, M. (1990). The rate of morphological evolution in mammals from the standpoint of the neutral expectation. *The American Naturalist, 136(6),* 727–741.

Machado, F. A. (2020). Selection and constraints in the ecomorphological adaptive evolution of the skull of living canidae (carnivora, mammalia). *The American Naturalist*, *196(2),* 197–215.

Machado, F. A., Zahn, T. M. G., & Marroig, G. (2018). Evolution of morphological integration in the skull of carnivora (mammalia): changes in canidae lead to increased evolutionary potential of facial traits. *Evolution*, *72*(7), 1399–1419. https://doi.org/10.1111/evo.13495

Machado, F. A., Hubbe, A., Melo, D., Porto, A., & Marroig, G. (2019). Measuring the magnitude of morphological integration: The effect of differences in morphometric representations and the inclusion of size. *Evolution*, *33*, 402–11.

Machado, F. A., Marroig, G., & Hubbe, A. (2022). The pre-eminent role of directional selection in generating extreme morphological change in glyptodonts (cingulata; xenarthra). *Proceedings*

Downloaded from academic.oup.com/evlett/advance-article/doi/10.1093/evlett/qrag039/8863744 by Maria Mestriner user on 30 October 2026

of the Royal Society B, 289(1967), 20212521. https://doi.org/10.1098/rspb.2021.2521

Machado, F. A., Mongle, C. S., Slater, G., Penna, A., Wisniewski, A., Soffin, A., Dutra, V., & Uyeda, J. C. (2023). Rules of teeth development align microevolution with macroevolution in extant and extinct primates. *Nature Ecology & Evolution*, *7*(10), 1729–1739. https://doi.org/10.1038/s41559-023-02167-w

Maestri, R., Monteiro, L. R., Fornel, R., Upham, N. S., Patterson, B. D., & de Freitas, T. R. O. (2017). The ecology of a continental evolutionary radiation: Is the radiation of sigmodontine rodents adaptive?, *Evolution*, *71*(3), 610–632. https://doi.org/10.1111/evo.13155

Marroig, G., & Cheverud, J. M. (2001). A comparison of phenotypic variation and covariation patterns and the role of phylogeny, ecology, and ontogeny during cranial evolution of new world monkeys. *Evolution*, *55*(12), 2576–2600. https://doi.org/10.1111/j.0014-3820.2001.tb00770.x

Marroig, G., & Cheverud, J. M. (2004). Did natural selection or genetic drift produce the cranial diversification of neotropical monkeys?, *The American Naturalist*, *163*(3), 417–428. https://doi.org/10.1086/381693

Marroig, G., & Cheverud, J. M. (2005). Size as a line of least evolutionary resistance: Diet and adaptive morphological radiation in new world monkeys. *Evolution*, *59*(5), 1128–1142. https://doi.org/10.1111/j.0014-3820.2005.tb01049.x

Marroig, G., & Cheverud, J. M. (2010). Size as a line of least resistance II: Direct selection on size or correlated response due to constraints?, *Evolution*, *64*(5), 1470–1488.

Marroig, G., Melo, D. A. R., & Garcia, G. R. G. (2012). Modularity, noise, and natural selection. *Evolution*, *66*(5), 1506–1524. https://doi.org/10.1111/j.1558-5646.2011.01555.x

Martin, L. D. (1980). Functional morphology and the evolution of cats. *Transactions of the Nebraska Academy of Sciences and Affiliated Societies, 8,* 141–153.

Martin, R. D. (1992). Goeldi and the dwarfs: The evolutionary biology of the small new world monkeys. *Journal of Human Evolution*, *22*(4-5), 367–393. https://doi.org/10.1016/0047-2484(92)90066-I

Masters, J. C., Génin, F., Silvestro, D., Lister, A. M., & DelPero, M. (2014). The red island and the seven dwarfs: body size reduction in cheirogaleidae. *Journal of Biogeography*, *41*(10), 1833–1847. https://doi.org/10.1111/jbi.12327

Melo, D., Garcia, G., Hubbe, A., Assis, A. P., & Marroig, G. (2015). Evolqg-an r package for evolutionary quantitative genetics. *F1000Research*, *4*. https://f1000research.com/articles/4-925/v3

Mitchell, K. J., Scanferla, A., Soibelzon, E., Bonini, R., Ochoa, J., & Cooper, A. (2016). Ancient DNA from the extinct South American giant glyptodont *Doedicurus* sp. (xenarthra: Glyptodontidae) reveals that glyptodonts evolved from eocene armadillos. *Molecular Ecology*, *25*(14), 3499–3508. https://doi.org/10.1111/mec.13695

Montgomery, S., & Mundy, N. (2013). Parallel episodes of phyletic dwarfism in callitrichid and cheirogaleid primates. *Journal of Evolutionary Biology*, *26*(4), 810–819. https://doi.org/10.1111/jeb.12097

Morgan, G. S., Czaplewski, N. J., & Simmons, N. B. (2019). A new mormoopid bat from the oligocene (whitneyan and early arikareean) of florida, and phylogenetic relationships of the major clades of mormoopidae (mammalia: Chiroptera). *Bulletin of the American Museum of Natural History*, *2019*(434), 1–146. https://doi.org/10.1206/0003-0090.434.1.1

Pacifici, M., Santini, L., Di Marco, M., Baisero, D., Francucci, L., Marasini, G. G., Visconti, P., & Rondinini, C. (2013). Generation length for mammals. *Nature Conservation*, *5*, 89–94.

Paijmans, J. L., Barnett, R., Gilbert, M. T. P., Zepeda-Mendoza, M. L., Reumer, J. W., de Vos, J., Zazula, G., Nagel, D., Baryshnikov, G. F., Leonard, J. A., Rohland, N., Westbury, M. V., Barlow, A., & Hofreiter, M. (2017). Evolutionary history of saber-toothed cats based on ancient mitogenomics. *Current Biology*, *27*(21), 3330–3336. https://doi.org/10.1016/j.cub.2017.09.033

Pavan, A., Wilson, D., & Mittermeier, R. (2019). Family mormoopidae (ghost-faced bats, naked-backed bats and mustached bats). *Handbook of the Mammals of the World*, *9*, 424–443.

Pavan, A. C., & Marroig, G. (2016). Integrating multiple evidences in taxonomy: Species diversity and phylogeny of mustached bats (mormoopidae: Pteronotus). *Molecular Phylogenetics and Evolution*, *103*, 184–198. https://doi.org/10.1016/j.ympev.2016.07.011

Pavan, A. C., & Marroig, G. (2017). Timing and patterns of diversification in the neotropical bat genus pteronotus (mormoopidae). *Molecular Phylogenetics and Evolution*, *108*, 61–69. https://doi.org/10.1016/j.ympev.2017.01.017

Percequillo, A. R., do Prado, J. R., Abreu, E. F., Dalapicolla, J., Pavan, A. C., de Almeida Chiquito, E., Brennand, P., Steppan, S. J., Lemmon, A. R., Lemmon, E. M., Lemmon, A. R., Moriarty, E., & Mark, W. (2021). Tempo and mode of evolution of oryzomyine rodents (rodentia, cricetidae, sigmodontinae): a phylogenomic approach. *Molecular Phylogenetics and Evolution*, *159*, 107120. https://doi.org/10.1016/j.ympev.2021.107120

Perini, F. A., Russo, C., & Schrago, C. G. (2010). The evolution of south american endemic canids: A history of rapid diversification and morphological parallelism. *Journal of Evolutionary Biology*, *23*(2), 311–322. https://doi.org/10.1111/j.1420-9101.2009.01901.x

Piras, P., Silvestro, D., Carotenuto, F., Castiglione, S., Kotsakis, A., Maiorino, L., Melchionna, M., Mondanaro, A., Sansalone, G., Serio, C., & Vero, V, Raia, P (2018). Evolution of the sabertooth mandible: A deadly ecomorphological specialization. *Palaeogeography, Palaeoclimatology, Palaeoecology*, *496*, 166–174. https://doi.org/10.1016/j.palaeo.2018.01.034

Polly, P. D. (2008). Adaptive zones and the pinniped ankle: A three-dimensional quantitative analysis of carnivoran tarsal evolution. In *Mammalian evolutionary morphology: A tribute to Frederick S. Szalay*,. (pp. 167–196), Dordrecht: Springer Netherlands.

Polly, P. D. (2024). Bear feet with björn: Tarsal evolution in the origin of polar bears. *Annales Zoologici Fennici, Vol. 61*. (pp. 357–376). BioOne.

Porto, A., Oliveira, F. B. d., Shirai, L. T., Conto, V., & Marroig, G. (2009). The evolution of modularity in the mammalian skull I: Morphological integration patterns and magnitudes. *Evolutionary Biology*, *36*(1), 118–135. https://doi.org/10.1007/s11692-008-9038-3

Porto, A., Sebastião, H., Pavan, S. E., VandeBerg, J. L., Marroig, G., & Cheverud, J. M. (2015). Rate of evolutionary change in cranial morphology of the marsupial genus *Monodelphisis* constrained by the availability of additive genetic variation. *Journal of Evolutionary Biology*, *28*(4), 973–985. https://doi.org/10.1111/jeb.12628

Downloaded from academic.oup.com/evlett/advance-article/doi/10.1093/evlett/qrag039/8863744 by Maria Mestriner user on 30 October 2026

Repenning, C. A. (1976). Adaptive evolution of sea lions and walruses. *Systematic Zoology*, *25*(4), 375–390. https://doi.org/10.2307/2412512

Rojas, D., Warsi, O. M., & Dávalos, L. M. (2016). Bats (chiroptera: Noctilionoidea) challenge a recent origin of extant neotropical diversity. *Systematic Biology*, *65*(3), 432–448. https://doi.org/10.1093/sysbio/syw011

Rolfe, A. K., Kurta, A., & Clemans, D. L. (2014). Species-level analysis of diets of two mormoopid bats from puerto rico. *Journal of Mammalogy*, *95*(3), 587–596. https://doi.org/10.1644/13-MAMM-A-190

Roseman, C. C. (2004). Detecting interregionally diversifying natural selection on modern human cranial form by using matched molecular and morphometric data. *Proceedings of the National Academy of Sciences*, *101*(35), 12824–12829. https://doi.org/10.1073/pnas.0402637101

Roseman, C. C., & Weaver, T. D. (2007). Molecules versus morphology? Not for the human cranium. *Bioessays*, *29*(12), 1185–1188. https://doi.org/10.1002/bies.20678

Rossoni, D. M., Assis, A. P. A., Giannini, N. P., & Marroig, G. (2017). Intense natural selection preceded the invasion of new adaptive zones during the radiation of new world leaf-nosed bats. *Scientific Reports*, *7*(1), 1–11. https://doi.org/10.1038/s41598-017-08989-6

Rossoni, D. M., Costa, B. M. A., Giannini, N. P., & Marroig, G. (2019). A multiple peak adaptive landscape based on feeding strategies and roosting ecology shaped the evolution of cranial covariance structure and morphological differentiation in phyllostomid bats. *Evolution*, *73*(5), 961–981. https://doi.org/10.1111/evo.13715

Rossoni, D. M., Patterson, B. D., Marroig, G., Cheverud, J. M., & Houle, D. (2024). The role of (co) variation in shaping the response to selection in new world leaf-nosed bats. *The American Naturalist*, *203*(4), E107–E127. https://doi.org/10.1086/729219

Ruiz, J. V., Ferreira, G. S., Lautenschlager, S., de Castro, M. C., & Montefeltro, F. C. (2023). Different, but the same: Inferring the hunting behaviour of the hypercarnivorous bush dog (speothos venaticus) through finite element analysis. *Journal of Anatomy*, *242*(4), 553–567. https://doi.org/10.1111/joa.13804

Schluter, D. (2024). Variable success in linking micro-and macroevolution. *Evolutionary Journal of the Linnean Society*, *3*(1), kzae016. https://doi.org/10.1093/evolinnean/kzae016

Schroeder, L., & Ackermann, R. R. (2017). Evolutionary processes shaping diversity across the homo lineage. *Journal of Human Evolution*, *111*, 1–17. https://doi.org/10.1016/j.jhevol.2017.06.004

Schroeder, L., & von Cramon-Taubadel, N. (2017). The evolution of hominoid cranial diversity: A quantitative genetic approach. *Evolution*, *71*(11), 2634–2649. https://doi.org/10.1111/evo.13361

Schroeder, L., Roseman, C. C., Cheverud, J. M., & Ackermann, R. R. (2014). Characterizing the evolutionary path (s) to early homo. *PloS One*, *9*(12), e114307. https://doi.org/10.1371/journal.pone.0114307

Silva-Neto, F. d. C., Pavan, S. E., & Astúa, D. (2024). Evolution, divergence, and convergence in the mandibles of opossums (didelphidae, didelphimorphia). *Current Zoology*, *70*(4), 488–504. https://doi.org/10.1093/cz/zoad027

Simpson, G. G. (1944). Tempo and mode in evolution. (15).

Simpson, G. G. (1953). The major features of evolution.

Slater, G. J., Figueirido, B., Louis, L., Yang, P., & Van Valkenburgh, B. (2010). Biomechanical consequences of rapid evolution in the polar bear lineage. *PLoS One*, *5*(11), e13870. https://doi.org/10.1371/journal.pone.0013870

Smith, H. F. (2011). The role of genetic drift in shaping modern human cranial evolution: A test using microevolutionary modeling. *International Journal of Evolutionary Biology*, *2011*(1), 145262.

Soto, E. C., Cañón, C., & Pardiñas, U. F. (2026). Undervalued habitat or impoverished guild? Explaining the scarcity of living semiaquatic sigmodontine rodents (cricetidae). *THERYA*, *17*(2), 327–342. https://doi.org/10.12933/therya.2026.6274

Tamagnini, D., Michaud, M., Meloro, C., Raia, P., Soibelzon, L., Tambusso, P. S., Varela, L., & Maiorano, L. (2023). Conical and sabertoothed cats as an exception to craniofacial evolutionary allometry. *Scientific Reports*, *13*(1), 13571. https://doi.org/10.1038/s41598-023-40677-6

Tulli, M. J., & Carrizo, L. V. (2024). From slenderness to robustness: Understanding long bone shape in sigmodontine rodents. *The Anatomical Record*, *307*(12), 3830–3849. https://doi.org/10.1002/ar.25521

Turelli, M., Gillespie, J. H., & Lande, R. (1988). Rate tests for selection on quantitative characters during macroevolution and microevolution. *Evolution*, *42*(5), 1085–1089. https://doi.org/10.1111/j.1558-5646.1988.tb02526.x

Uyeda, J. C., Hansen, T. F., Arnold, S. J., & Pienaar, J. (2011). The million-year wait for macroevolutionary bursts. *Proceedings of the National Academy of Sciences of the United States of America*, *108*(38), 15908–15913. https://doi.org/10.1073/pnas.1014503108

Van Valen, L. (1971). Adaptive zones and the orders of mammals. *Evolution*, *25,* 420–428. https://doi.org/10.1111/j.1558-5646.1971.tb01898.x

Van Valkenburgh, B. (1991). Iterative evolution of hypercarnivory in canids (mammalia: Carnivora): Evolutionary interactions among sympatric predators. *Paleobiology*, *17*(4), 340–362. https://doi.org/10.1017/S0094837300010691

Vizcaíno, S. F., Cassini, G. H., Fernicola, J. C., & Bargo, M. S. (2011). Evaluating habitats and feeding habits through ecomorphological features in glyptodonts (mammalia, xenarthra). *Ameghiniana*, *48*(3), 305–319. https://doi.org/10.5710/AMGH.v48i3(364)

Voje, K. L., Saulsbury, J. G., Starrfelt, J., Latorre, D. V., Rojas, A., Kinneberg, V. B., Liow, L. H., Wilson, C. J., Saupe, E. E., & Grabowski, M. (2023). Measurement theory and paleobiology. *Trends in Ecology & Evolution*, *38*(12), 1165–1176. https://doi.org/10.1016/j.tree.2023.08.005

Weaver, T. D., & Stringer, C. B. (2015). Unconstrained cranial evolution in neandertals and modern humans compared to common chimpanzees. *Proceedings of the Royal Society B: Biological Sciences*, *282*(1817), 20151519. https://doi.org/10.1098/rspb.2015.1519

Weaver, T. D., Roseman, C. C., & Stringer, C. B. (2007). Were neandertal and modern human cranial differences produced by natural selection or genetic drift?, *Journal of Human Evolution*, *53*(2), 135–145. https://doi.org/10.1016/j.jhevol.2007.03.001

Weaver, T. D., Roseman, C. C., & Stringer, C. B. (2008). Close correspondence between quantitative-and molecular-genetic divergence times for neandertals and modern humans. *Proceed-*

Downloaded from academic.oup.com/evlett/advance-article/doi/10.1093/evlett/qrag039/8863744 by Maria Mestriner user on 30 October 2026

ings of the National Academy of Sciences, *105*(12), 4645–4649. https://doi.org/10.1073/pnas.0709079105

Wilder, A. P., Supple, M. A., Subramanian, A., Mudide, A., Swofford, R., Serres-Armero, A., Steiner, C., Koepfli, K. P., Genereux, D. P., Karlsson, E. K., Lindblad-Toh, K., Marques-Bonet, T., Fuentes, V. M., Foley, K., Meyer, W. K., Consortium, Z., Ryder, O. A., & Shapiro, B. (2023). The contribution of historical processes to contemporary extinction risk in placental mammals. *Science*, *380*(6643), eabn5856. https://doi.org/10.1126/science.abn5856

Wisniewski, A. L., Lloyd, G. T., & Slater, G. J. (2022). Extant species fail to estimate ancestral geographical ranges at older nodes in primate phylogeny. *Proceedings of the Royal Society B*, *289*(1975), 20212535. https://doi.org/10.1098/rspb.2021.2535

Downloaded from academic.oup.com/evlett/advance-article/doi/10.1093/evlett/qrag039/8863744 by Maria Mestriner user on 30 October 2026

Received: 24 December 2025. **Revised:** 18 July 2026. **Accepted:** 14 August 2026

© The Author(s) 2026. Published by Oxford University Press on behalf of The Society for the Study of Evolution (SSE) and European Society for Evolutionary Biology (ESEB).
This is an Open Access article distributed under the terms of the Creative Commons Attribution-NonCommercial License (https://creativecommons.org/licenses/by-nc/4.0/), which permits non-commercial re-use, distribution, and reproduction in any medium, provided the original work is properly cited. For commercial re-use, please contact reprints@oup.com for reprints and translation rights for reprints. All other permissions can be obtained through our RightsLink service via the Permissions link on the article page on our site-for further information please contact journals.permissions@oup.com